C. R. Chimie 19 (2016) 475–485

Contents lists available at ScienceDirect

Comptes Rendus Chimie

www.sciencedirect.com

Full paper/Mémoire

Synthesis of EMT/FAU-type zeolite nanocrystal aggregates in high yield and crystalline form

Synthèse d'agrégats de nanocristaux de zéolithe de type EMT/FAU avec un rendement et un état cristallin élevés

Laetitia Bullot [a, b], T. Jean Daou [a, *], Angélique Simon-Masseron [a], Gérald Chaplais [a], Joël Patarin [a, **]

[a] *Université de Strasbourg (UDS), Université de Haute Alsace (UHA), Equipe Matériaux à Porosité Contrôlée (MPC), Institut de Science des Matériaux de Mulhouse (IS2M), UMR CNRS 7361, ENSCMu, 3B, rue Alfred-Werner, 68093 Mulhouse Cedex, France*
[b] *French Environment and Energy Management Agency, 20 avenue du Grésillé, BP 90406 49004 Angers Cedex 01, France*

ARTICLE INFO

Article history:
Received 27 May 2015
Accepted 5 October 2015
Available online 5 February 2016

Keywords:
Zeolite
EMT-type zeolite
FAU-type zeolite
Nanocrystal aggregates
Synthesis yield
Crystallization rate

ABSTRACT

This work focuses on different ways to improve the yield and/or the crystalline quality of EMT/FAU-type zeolite nanocrystal aggregates obtained in the presence of organic additive triethanolamine (TEA). The increase of the amount of aluminum reagent enhances the synthesis yield by a factor of 2.5 without affecting the crystallization rate and the microporous volume. On the other hand, the increase of the thermal treatment time allows to increase the synthesis yield, the crystallization rate and the microporous volume. Furthermore, addition of EMT zeolite seeds into the starting reaction medium improves the crystallization rate and the microporous volume.

Mots-clés:
Zéolithe
Zéolithe de type EMT
Zéolithe de type FAU
Agrégats nanocristallins
Rendement de la synthèse
Taux de cristallisation

RÉSUMÉ

Ce travail est centré sur les différentes façons d'améliorer le rendement et/ou l'état cristallin d'agglomérats de nanocristaux de zéolithe de type EMT/FAU obtenus en présence de triéthanolamine (TEA). L'augmentation de la quantité de la source d'aluminium permet d'augmenter le rendement par un facteur 2,5 sans affecter le taux de cristallisation et le volume microporeux. Par ailleurs, l'augmentation de la durée du traitement thermique entraîne une augmentation du rendement, du taux de cristallisation et du volume microporeux. L'ajout de germes de zéolithe EMT dans le milieu réactionnel de départ permet d'améliorer le taux de cristallisation et le volume microporeux.

1. Introduction

Zeolites are crystalline aluminosilicate materials with controlled porosity. They are composed of TO_4 tetrahedra

* Corresponding author.
** Corresponding author.
E-mail addresses: laetitia.bullot@uha.fr (L. Bullot), jean.daou@uha.fr (T.J. Daou), angelique.simon-masseron@uha.fr (A. Simon-Masseron), gerald.chaplais@uha.fr (G. Chaplais), joel.patarin@uha.fr (J. Patarin).

http://dx.doi.org/10.1016/j.crci.2015.10.012

combinations, where T is either silicon or aluminum elements. These materials present several characteristics such as a high thermal stability [1,2], a high porous volume and a high specific surface area [3–5]. Due to these excellent properties, zeolite materials have been recognized as promising candidates for multifunctional applications such as catalysis, ion-exchange, gas separation, etc [6–12]. In addition, zeolite materials are also of scientific and technological importance because of their ability to adsorb and interact with atoms and molecules [13–17]. Among all the zeolite structures, EMT- and FAU- type zeolites are very interesting due to their large pore and cage sizes that give them great potential as sorption materials [18]. They also display high thermal and hydrothermal stabilities and present excellent catalytic activity [19–21]. In both cases, the structures are constituted by sodalite cages linked through double six-rings (D6R). EMT zeolite is commonly known as the hexagonal analog of faujasite. Its structure results from a stacking of faujasite sheets connected through D6R units by a mirror plane symmetry operation whereas, in the case of faujasite, the connection occurs through an inversion center symmetry operation [21–23]. Such an assembly allows the formation of two types of cages: a larger hypercage (1.24 nm^3) and a smaller ellipsoid hypocage (0.61 nm^3) [22,23]. The synthesis of high silica EMT-type zeolite commonly named EMC-2 (Elf Mulhouse Chemistry Two) was reported by Guth and co-workers [24,25]. They were the first to synthesize the hypothetical so-called Breck Six Structure (EMT-type structure), with a silicon to aluminum molar ratio between 3 and 5, by using the 18-crown-6 ether as the structure-directing agent (SDA). The similarity between the FAU- and EMT-type structures leads to a large number of EMT/FAU-type intergrowths such as ZSM-3, ZSM-20, ECR-30, CSZ-1 and CSZ-3 materials [26].

Very recently, Mintova and co-workers managed to develop new SDA-free synthesis routes for EMC-2 zeolite nanoparticles from a Na-rich colloidal suspension at a low temperature (30 °C) after 36 h of thermal treatment. The obtained crystals have a silicon to aluminum molar ratio of about 1.1 and crystal sizes ranging from 6 to 15 nm [27]. This low silicon to aluminum molar ratio could be really interesting for some applications such as adsorption of organic molecules. Recently, the effect of organic additive triethanolamine (TEA) on the crystallization process of EMT-type zeolite nanocrystals to enable their easy filtration for industrial applications was investigated by our group [28]. The addition of 5 equivalents of TEA additives (for 1 eq. of Al_2O_3 and 5 eq. of SiO_2) to the zeolite EMC-2 nanocrystal synthesis gel leads to the formation of larger and aggregated crystals around 1 μm in size. These agglomerated crystals were composed of EMT/FAU zeolitic nanosheets/nanoplatelets (30–60 nm in thickness) displayed in a house-of-cards-like assembly with wide macroporous interstices between the nanosheet/nanoplatelet stacking. This type of morphology has already been highlighted by Inayat et al. with the assembly of mesoporous FAU-type zeolite nanosheets [29].The obtained aggregated crystals can be easily recovered by filtration from the synthesis medium and washed [28]. Indeed, without this agglomeration, nanocrystals were impossible to filter which represents a real constraint for a large scale synthesis. The agglomeration method relies on the introduction of an organic molecule “TEA” which acts as a stabilizing and complexing agent for aluminum with the agglomeration of the crystals [30–34]. Because of its chelating property with Al^{3+}, TEA has the ability to form a robust monometric tricyclic complex [33,34]. However, a drastic reduction of the synthesis yield was observed when this complexing agent was added. This reduction is explained by the fact that a part of the introduced aluminum is complexed by the TEA molecules and therefore does not react with the silicon to form the zeolite. Scott and co-workers have suggested that TEA may reduce the concentration of “free aluminum” in the gel synthesis and act as an “aluminum scavenger” which is coherent with our results [30,31]. This decrease in the synthesis yield is a barrier for an industrial production. Consequently, this work is undertaken to find solutions to increase the EMT/FAU-type zeolite aggregate yield. As a first alternative an increase of the sodium aluminate content introduced into the starting synthesis medium in order to enlarge the amount of aluminum used to form zeolite is considered. Another solution is to extend the thermal treatment time while avoiding the formation of non-desired phases such as GIS or SOD-type zeolites. The third possibility is based on a seeding process using EMT-type conventional big crystals and nanocrystals in order to accelerate the crystallization kinetics.

2. Experimental part

2.1. Syntheses of EMT-type zeolite nanocrystal aggregates

2.1.1. Influence of the starting aluminum concentration and the thermal treatment time (studies A and B)

The reaction mixture was obtained following the protocol described in our previous paper [28], which allows to obtain EMT/FAU nanocrystal aggregates from a Na-rich precursor suspension at 30 °C and in the presence of 5 equivalents of triethanolamine ($TEA/Al_2O_3 = 5$).

The syntheses were performed using polypropylene bottles. First, a certain amount of sodium hydroxide (Riedel-de-Haën; 98%) was homogenized in 61.60 g of deionized water. Then, a certain amount (2.04–4.63 g) of sodium aluminate (Strem Chemicals: 56.7% Al_2O_3 and 39.5% Na_2O) was added under magnetic stirring until the solution became completely clear. 12.64 g of sodium silicate (Sigma–Aldrich, 26.5% SiO_2, 10.6% Na_2O) were then added under vigorous stirring. After 10 min of magnetic stirring a milky solution is obtained. Finally, 5 equivalents of TEA additive (Acros Organic, 99%) were added to the gel under magnetic stirring. After 5 min of magnetic stirring a clear solution was obtained with the following molar composition: 5 SiO_2: x Al_2O_3: 17.5 Na_2O: y TEA: 340 H_2O with $x = 1$, 1.5, 1.67, 2 or 2.67 and $y = 0$ or 5 (x and y being the molar composition in the starting synthesis medium of Al_2O_3 and TEA, respectively). The obtained clear solution was then left at room temperature for 15 h under magnetic stirring prior to heating at 30 °C for z days with $z = 7$, 15 or 42 days (z being the thermal treatment time). After the synthesis, the products were filtered or centrifuged (depending on the size of EMT/FAU aggregates) and then washed with

deionized water several times. The obtained solids were then dried under vacuum at −80 °C using a lyophilizer. In study A, related to the influence of the aluminum concentration in the started synthesis medium, x changed while *y* and *z* were fixed at 5 and 7, respectively. In study B, related to the influence of the thermal treatment time, *z* changed while *x* and *y* were fixed at 1 and 5, respectively.

2.1.2. Influence of the introduction of EMT crystals as seeds into the starting synthesis medium (study C)

The same protocol as the previous one was used for this study (with $x = 1$, $y = 5$ and $z = 7$). Two types of EMT zeolite crystals were used as seeds in order to enhance the crystallization kinetics: i) conventional big EMT zeolite crystals with a regular hexagonal platelet morphology of 2 μm and a Si to Al molar ratio of 3.9 (denoted hereafter as B), and ii) EMT nanocrystals synthesized as shown above without TEA ($y = 0$) with particle sizes ranging from 6 to 15 nm and a Si to Al molar ratio of 1.1 (denoted hereafter as N). 2 or 4 wt % of EMT particles relative to the SiO_2 amount were introduced into the synthesis medium (the final molar composition of silica was kept unchanged).

Hereafter the different zeolite samples obtained from the studies A, B and C will be defined as $S_{x;y;z;w}$, where *w* represents the weight percentage of the introduced seeds (2 or 4) and their particle size (N for nanocrystals and B for big crystals).

2.2. Characterization

The purity and the crystallinity of the synthesized products were checked by X-ray diffraction (XRD) analysis. XRD patterns of the different samples were recorded using a PANalytical MPD X'Pert Pro diffractometer operating with Cu Kα radiation ($\lambda = 0.15418$ nm) equipped with an X'Celerator real-time multiple strip detector (active length = 2.122° 2θ). The powder pattern was collected at 22 °C in the range of $3 < 2\theta < 50°$ with a 2θ angle step of 0.017° and a time step of 220 s.

The size and the morphology of the crystals were determined by Scanning Electron Microscopy (SEM) using a Philips XL 30 FEG microscope and by Transmission Electron Microscopy (TEM) using a Philips model CM200, under an acceleration voltage of 200 kV, with a point-to-point resolution of 0.3 nm.

Nitrogen adsorption/desorption isotherms were measured using a Micromeritics ASAP 2420 apparatus. Prior to the adsorption measurements, the samples were outgassed at 300 °C overnight under vacuum. The specific surface area (S_{BET}) and microporous volume (V_{micro}) were calculated using the BET and *t*-plot methods, respectively. The mesoporous volume (V_{meso}) was calculated using the BJH method. The crystallization rates of the different synthesized samples were deduced from their microporous volumes considering that 100% of crystallized EMC-2 and NaX zeolite samples both present a microporous volume of 0.33 cm^3/g [21].

The Si/Al molar ratios of the synthesized samples were estimated by X-Ray Fluorescence spectrometry (Philips, Magic X).

The synthesis yields relative to silicon and aluminum were determined from the mass of the zeolite obtained and those of the silicon and aluminum introduced into the starting mixture. These yields were also confirmed by the residual amounts of silicon and aluminum in mother liquor which were determined by atomic absorption spectrometry using a Varian A.A 240 FS atomic absorption spectrometer. As a radiation source, hollow cathode lamps of Al and Si were used. The corresponding wavelengths and applied electric currents were: $\lambda_{Al} = 309.3$ nm, $I_{Al} = 10$ mA and $\lambda_{Si} = 251.6$ nm, $I_{Si} = 10$ mA. In both cases, a N_2O-acetylene flame with flow rates of 11 and 8.0 L/min, respectively, was used for the analyses.

3. Results

Peaks indexation of XRD patterns of each sample synthesized in this study revealed the presence of both EMT and FAU (NaX) crystalline phases (see Fig. S1). As shown in our previous paper [28], the quantification of these crystalline phases can be achieved using the method developed by Treacy et al. [35]. This method is based on a computer algorithm simulating the X-ray diffractograms of several EMT and FAU crystalline phase mixtures. For most of the products synthesized in this study, the estimated proportion of crystalline phases of EMC-2 (EMT-type) and NaX (FAU-type) zeolites are estimated at 70% and 30%, respectively (see Table 1). However, when the crystallization time increases, richer FAU-type materials are obtained with an estimated proportion of FAU close to 50% (after 15 days) and 70% (after 42 days).

3.1. Influence of the aluminum concentration in the starting synthesis medium: study A

Samples obtained from a starting synthesis medium with a molar composition of Al_2O_3 greater than 1 revealed a slightly lower crystallization rate compared to the sample synthesized with 1 equivalent of Al_2O_3 (see Fig. 1). Indeed, XRD patterns show broader and less intense peaks when the *x* value exceeded 1 which reflects a decrease in the crystal size. This result was confirmed by TEM and SEM observations which reveal that the size of EMT/FAU aggregates decreases while increasing the molar composition of Al_2O_3 in the starting synthesis medium (see Fig. 2). Zeolite aggregates with an average size of 1 μm were obtained when *x* was fixed at 1 while aggregates around 0.2–0.4 μm were observed when the value of *x* exceeded 1

Table 1
Crystalline phase quantification of the synthesized zeolite samples.

Samples	EMT-type zeolite estimated proportion[a] (%)	FAU-type zeolite estimated proportion[a] (%)
$S_{1;5;7;0}$	70	30
$S_{1;5;15;0}$	50	50
$S_{1;5;42;0}$	30	70
$S_{1;5;7;2N}$	70	30
$S_{1;5;7;4N}$	60	40
$S_{1;5;7;2B}$	80	20
$S_{1;5;7;4B}$	60	40

[a] According to the method proposed by Treacy et al. [34].

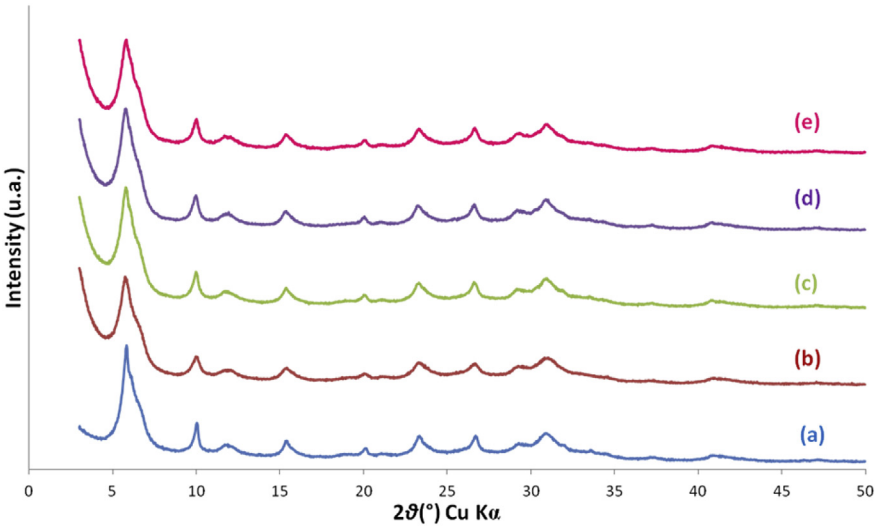

Fig. 1. XRD patterns of the zeolite samples synthesized in the presence of 5 equivalents of TEA additive with 1 equivalent ((a), $S_{1;5;7;0}$), 1.5 equivalents ((b), $S_{1.5;5;7;0}$), 1.67 equivalents ((c), $S_{1.67;5;7;0}$), 2 equivalents ((d), $S_{2;5;7;0}$) and 2.27 equivalents ((e), $S_{2.27;5;7;0}$) of Al_2O_3 after 7 days of thermal treatment at 30 °C.

(see Fig. 2). The more the value of *x* increases, the less aggregates were visible. This phenomenon could be explained by a higher amount of free aluminum species in the starting synthesis medium.

This observation was also confirmed by the fact that the filtration step became impossible to realize when the molar composition of Al_2O_3 in the starting synthesis medium exceeded 1. Syntheses carried out by increasing the amount of alumina (relative to the base composition: 1 equivalent of Al_2O_3) were in the form of unfilterable viscous gel like syntheses without TEA. Thus, the amount of TEA was insufficient to allow a complete aggregation of the crystals when x exceeded 1.

The silicon to aluminum molar ratios of the obtained samples from the study A were still unchanged (Si/Al = 1.1).

Nitrogen adsorption–desorption isotherms at 77 K of the zeolite samples synthesized in the presence of 5 equivalents of TEA additive in the synthesis medium and with different amounts of Al_2O_3 are presented in Fig. 3.

A type I isotherm, characteristic of purely microporous materials, is observed when 1 equivalent of Al_2O_3 was added to the initial synthesis medium (see Fig. 3a, $S_{1;5;7;0}$). When *x* exceeded 1 equivalent, the isotherms of the product obtained show a hysteresis loop (high N_2 uptake) at high relative pressures revealing an intergrain porosity as already observed for the EMT zeolite sample synthesized in the absence of TEA [28]. In agreement with the SEM and TEM results described above, this intergrain porosity confirms the presence of very small zeolite particles. Microporous volumes were substantially equal regardless of the value of *x* (see Table 2). The crystallization rates deduced from the microporous volume compared to fully crystallized EMC-2 and NaX zeolite samples were between 55 and 60%. The external surface area of the obtained samples increased when *x* exceeded 1. This result is in good agreement with the decrease of zeolite aggregate size observed above.

However, an increase of the Al_2O_3 molar composition in the starting synthesis medium allows us to increase the synthesis yield relative to silicon and aluminum (see Table 3).

When the amount of Al_2O_3 was doubled, the yield relative to aluminum was multiplied by 2.6 and the yield relative to silicon was almost increased by a factor of 4.9. This allows to increase the amount of product obtained, and thus to reduce the loss of reactants (aluminate and sodium silicate) observed in the synthesis of $S_{1;5;7;0}$. This result was confirmed by atomic absorption spectroscopy which revealed a decrease in the amount of silicon in the mother liquor when the amount of aluminum increased (see Table S1).

3.2. *Influence of the thermal treatment time: study B*

XRD patterns of the samples synthesized with different thermal treatment times reveal a better crystallization rate when this time is extended. Diffraction peaks are more clearly defined (sharper and more intense), revealing a higher crystallization rate for the sample synthesized with a thermal treatment time of 15 ($S_{1;5;15;0}$) and 42 days ($S_{1;5;42;0}$) as will be confirmed below by N_2 adsorption–desorption results (see Fig. 4).

However as mentioned above, the presence of both EMT and FAU phases or EMT/FAU intergrowths is clearly evidenced. The proportion of FAU-type zeolite in the samples obtained increases with the duration of the thermal treatment and reaches 70% after 42 days of thermal treatment (see Table 1).

SEM and TEM images presented in Fig. 5 show an increase in the particle size while increasing the thermal treatment time. Zeolitic nanosheets/nanoplatelets (30–60 nm in thickness) composing the aggregates obtained after 7 days ($S_{1;5;7;0}$) of thermal treatment were progressively transformed to a mixture of hexagonal crystals characteristic of the EMT-type zeolite and bipyramidal

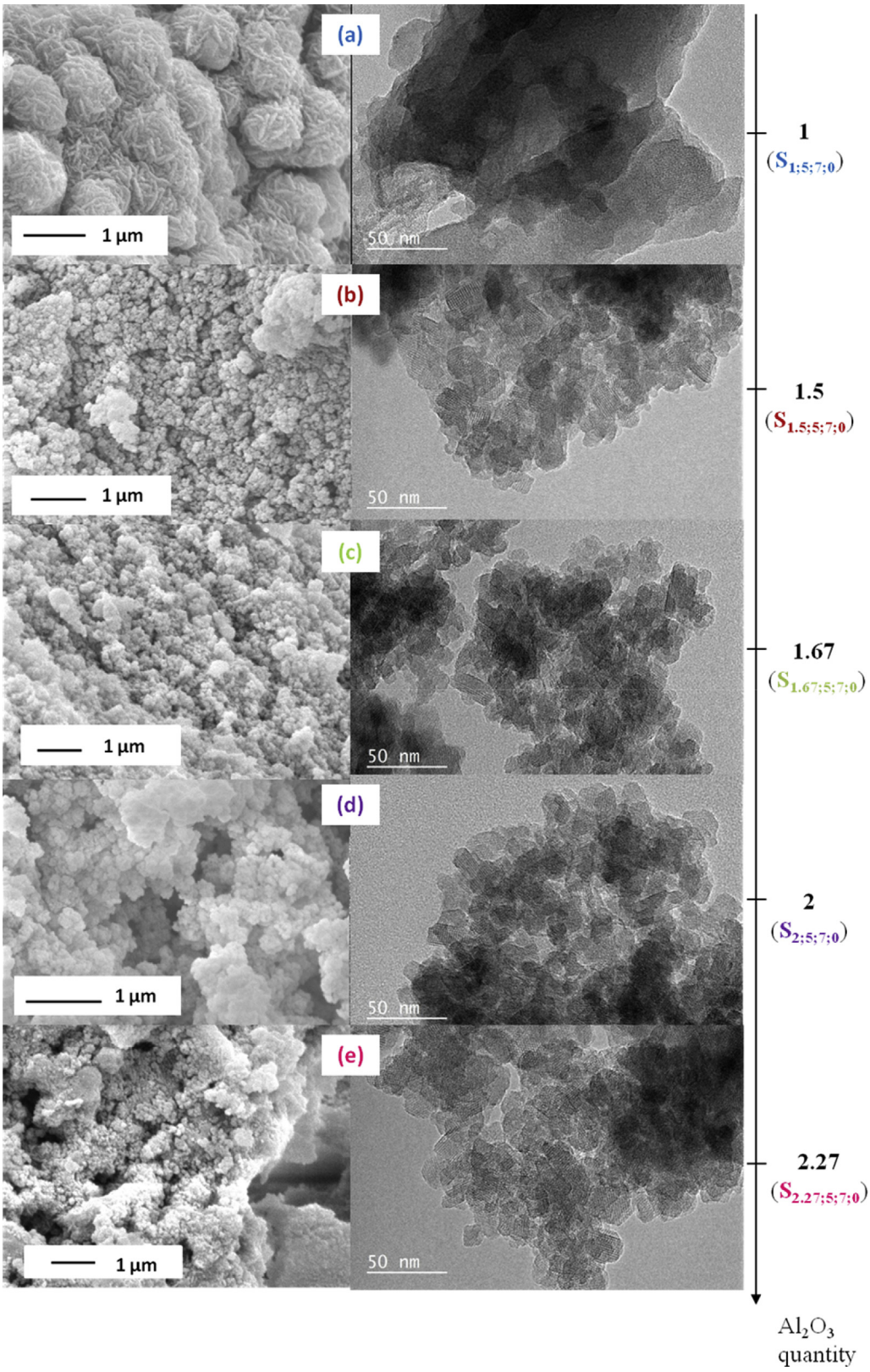

Fig. 2. SEM images (on the left) and TEM images (on the right) of the zeolite samples synthesized in the presence of 5 equivalents of TEA additive with 1 equivalent ((a), $S_{1;5;7;0}$), 1.5 equivalents ((b), $S_{1.5;5;7;0}$), 1.67 equivalents ((c), $S_{1.67;5;7;0}$), 2 equivalents ((d), $S_{2;5;7;0}$) and 2.27 equivalents ((e), $S_{2.27;5;7;0}$) of Al_2O_3 after 7 days of thermal treatment at 30 °C.

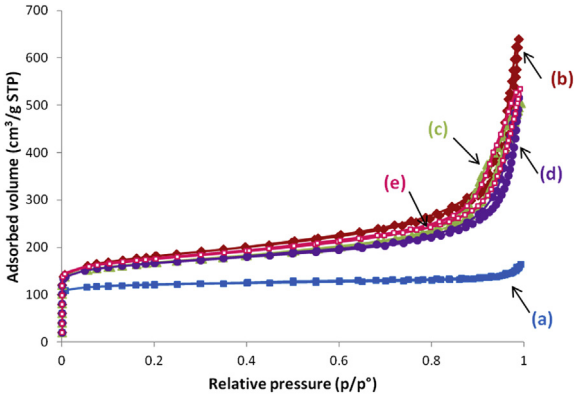

Fig. 3. Nitrogen adsorption–desorption isotherms at 77 K of the zeolite samples synthesized in the presence of 5 equivalents of TEA additive with 1 equivalent ((a) full square, $S_{1;5;7;0}$), 1.5 equivalents ((b) full diamond, $S_{1.5;5;7;0}$), 1.67 equivalents ((c) full triangle, $S_{1.67;5;7;0}$), 2 equivalents ((d) full circle, $S_{2;5;7;0}$) and 2.27 equivalents ((e) empty square, $S_{2.27;5;7;0}$) of Al_2O_3 after 7 days of thermal treatment at 30 °C.

crystals characteristic of the FAU-type zeolite with an average size of 150 nm and 500 nm for the samples $S_{1;5;15;0}$ and $S_{1;5;42;0}$, respectively (see Fig. 5). Filtration was possible regardless of the crystallization time.

The increase of the thermal treatment time did not affect the silicon to aluminum molar ratio of the obtained samples (Si/Al = 1.1).

Type I isotherms, characteristic of purely microporous materials, are observed for samples $S_{1;5;15;0}$ and $S_{1;5;42;0}$ (see Fig. 6). This increase in the thermal treatment time allowed an increase in the microporous volume (see Table 2). Crystallization rates were increased by 45% when increasing the thermal treatment time from 7 to 42 days. This result correlates with the one observed by XRD and represents a real advantage for some applications especially for molecular decontamination.

Like in study A, the synthesis yields relative to silicon and aluminum increase with the thermal treatment time as shown in Table 3. In comparison with those of sample $S_{1;5;7;0}$, these yields were almost multiplied by 2 and 2.5 for the samples $S_{1;5;15;0}$ and $S_{1;5;42;0}$, respectively.

Table 3
Synthesis yield of the obtained zeolite samples.

Samples	Yield relative to silicon (%)	Yield relative to aluminium (%)
$S_{1;5;7;0}$	9	19
$S_{1.5;5;7;0}$	24	31
$S_{1.67;5;7;0}$	38	51
$S_{2;5;7;0}$	44	50
$S_{2.27;5;7;0}$	54	53
$S_{1;5;15;0}$	16	36
$S_{1;5;42;0}$	21	48
$S_{1;5;7;\ 2B}$	6	11
$S_{1;5;7;\ 4B}$	12	21
$S_{1;5;7;\ 2N}$	4	9
$S_{1;5;7;\ 4N}$	9	17

3.3. *Influence of the introduction of EMT calcined crystals as seeds into the starting synthesis medium: study C*

Zeolite crystals are commonly introduced as seeds in synthesis media in order to increase the kinetics of crystallization [36–39]. The aim of this study was to determine the impact of the addition of EMT-type zeolite calcined seeds on the synthesis yield and the crystallization rate of the EMT/FAU-type zeolite aggregates obtained. The XRD patterns of the four zeolite samples synthesized in the presence of 2 or 4 wt % (relative to the amount of silica) of EMT seeds revealed the absence of other crystalline phases (see Fig. 7). The XRD patterns of the samples obtained in the presence of 4 wt % of seeds present more defined peaks which can be a sign of an increase in the crystallization rate as will be shown below with the nitrogen adsorption–desorption results. However, according to the synthesis yields relative to silicon which are quite low (9% with nanocrystals and 12% with big crystals, see Table 3), the relative proportion of seeds in the obtained product, if they are not dissolved during the thermal treatment, is therefore quite high and the better quality of the XRD patterns can be

Table 2
Textural properties of the zeolite samples.

Samples	S_{BET}[a] (m^2/g)	S_{ext}[b] (m^2/g)	V_{micro}[c] (cm^3/g)	V_{meso}[d] (cm^3/g)	Estimated crystallization rate[e] (%)
$S_{1;0;7;0}$	600	228	0.17	0.80	50
$S_{1;5;7;0}$	471	20	0.18	/	55
$S_{1.5;5;7;0}$	614	222	0.18	0.65	55
$S_{1.67;5;7;0}$	597	170	0.19	0.55	60
$S_{2;5;7;0}$	634	154	0.19	0.54	60
$S_{2.27;5;7;0}$	623	185	0.19	0.59	60
$S_{1;5;15;0}$	653	15	0.23	/	70
$S_{1;5;42;0}$	774	10	0.27	/	80
$S_{1;5;7;2N}$	395	11	0.15	/	45
$S_{1;5;7;4N}$	628	23	0.23	/	70
$S_{1;5;7;2B}$	414	8	0.15	/	45
$S_{1;5;7;4B}$	721	13	0.27	/	80

[a] S_{BET}: specific surface area.
[b] S_{ext}: external surface area.
[c] V_{micro}: micropore volume (determined by the t-plot method).
[d] V_{meso}: mesopore volume (determined by the BJH method).
[e] Estimated crystallization rate deduced from V_{micro} considering a micropore volume of 0.33 cm^3/g for 100% crystallized EMC-2 and NaX zeolite samples.

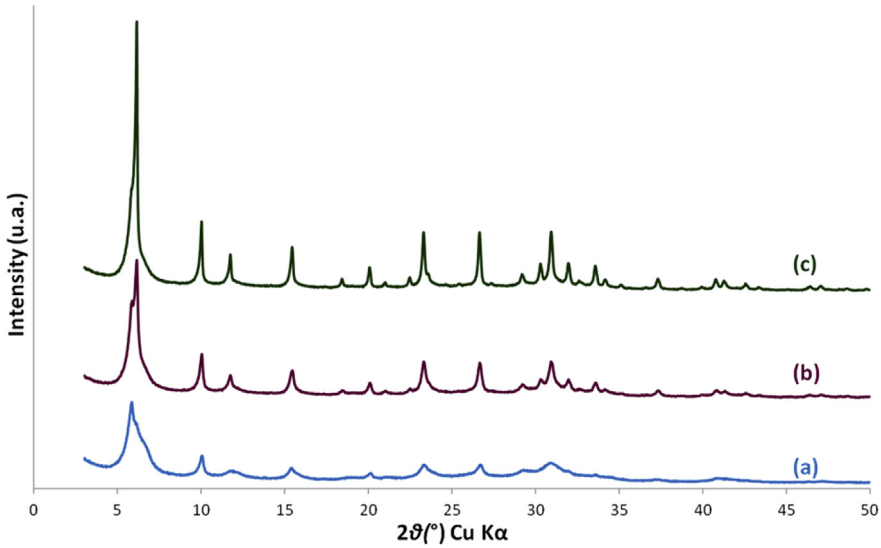

Fig. 4. XRD patterns of the zeolite samples synthesized in the presence of 5 equivalents of TEA additive after 7 days ((a), $S_{1;5;7;0}$), 15 days ((b), $S_{1;5;15;0}$) and 42 days ((c), $S_{1;5;42;0}$) of thermal treatment at 30 °C.

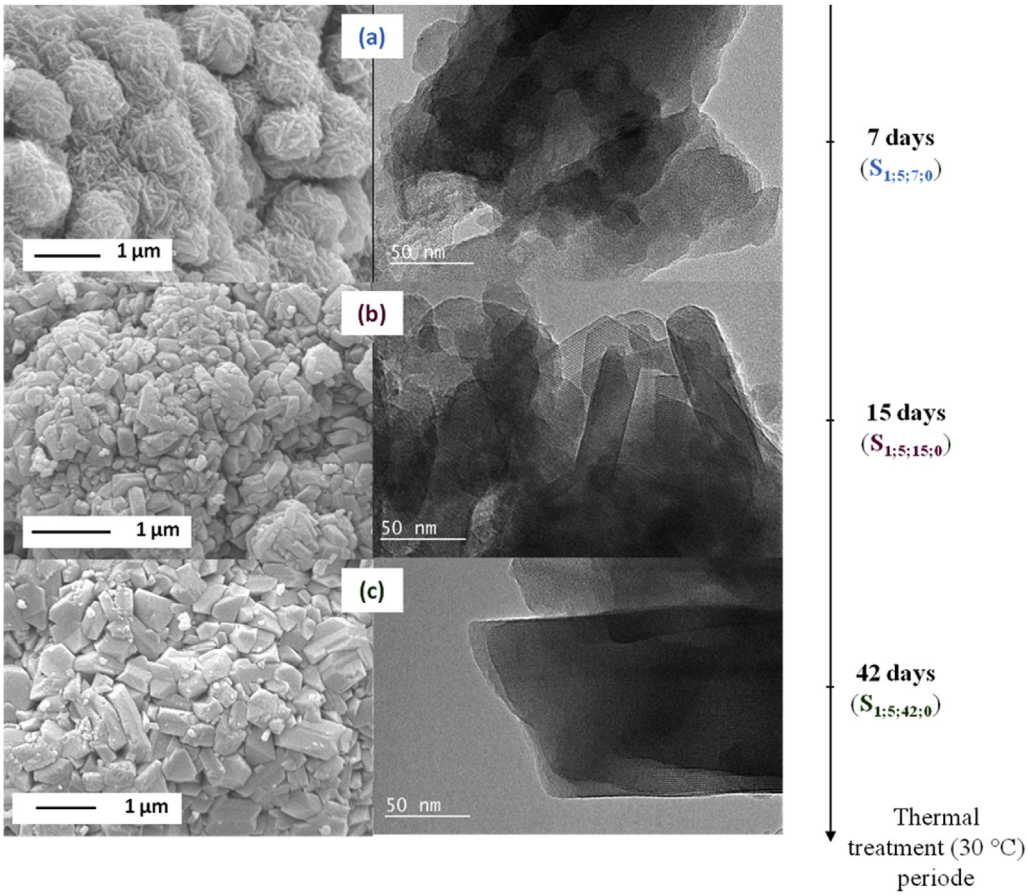

Fig. 5. SEM images (on the left) and TEM images (on the right) of the zeolite samples synthesized in the presence of 5 equivalents of TEA additive after 7 days ((a), $S_{1;5;7;0}$), 15 days ((b), $S_{1;5;15;0}$) and 42 days ((c), $S_{1;5;42;0}$) of thermal treatment at 30 °C.

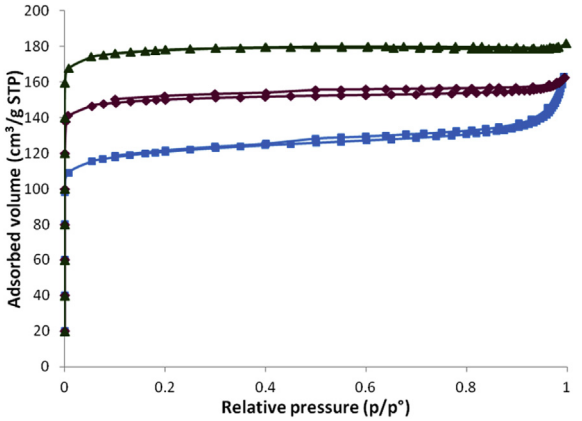

Fig. 6. Nitrogen adsorption–desorption isotherms at 77 K of the zeolite samples synthesized in the presence of 5 equivalents of TEA additive after 7 days (full square, $S_{1;5;7;0}$), 15 days (full diamond, $S_{1;5;15;0}$) and 42 days (full triangle, $S_{1;5;42;0}$) of thermal treatment at 30 °C.

due to the presence of seeds. Such a hypothesis seems to be confirmed, at least for the sample $S_{1;5;7;4B}$, (big crystal seeds), by the apparition of an additional characteristic diffraction peak of the EMT-type zeolite at $2\theta = 10.55°$ (see * in Fig. 7).

Surprisingly, compared to that of the non-seeded sample ($S_{1;5;7;0}$), the crystalline phase quantification determined by the Treacy et al. method [35] indicates a higher proportion of FAU-type zeolite (40% instead of 30%) (see Table 1). Normally, seeding crystals of a particular zeolite phase are used to favor the production of this particular phase [40–42].

In contrast, the introduction of only 2 wt % of zeolite seeds appears not to be enough to increase the crystallization kinetics and the proportion of FAU is close to 20–30% (see Table 1).

SEM and TEM images (see Fig. 8) show that, when conventional big EMT crystals are used as seeds, the size of aggregates increases slightly to about 1.5–2 μm, which represents exactly the size of the conventional big EMT crystal seeds.

Therefore, the EMT/FAU nanosheets/nanoplatelets seem to grow on original seed crystals.

However, the Si/Al molar ratio of the seeded samples was always unchanged (Si/Al = 1.1) which means that a biggest part of the seed crystals has been used as the raw material for the crystallization of EMT/FAU nanosheets/nanoplatelets.

Nitrogen adsorption–desorption experiments performed on the zeolite samples synthesized in the presence of EMT seeds show type I isotherms characteristic of microporous materials with an even more flat plateau than the one obtained for the sample prepared in the absence of seeds (see Fig. 9). According to the micropore volume, crystallization rates increase by 28% and 50% compared to the $S_{1;5;7;0}$ sample when 4 wt % of EMT nanocrystals or EMT big crystals are used, respectively (see Table 2).

$S_{1;5;7;4N}$ and $S_{1;5;7;4B}$ samples obtained with the introduction of 4 wt % of seeds present higher microporous volumes than samples synthesized with 2 wt % of similar seeds (see Table 2).

The trend in crystallization rates deduced from microporous volumes corroborates the observation made above by XRD analyses. Microporous volumes remain slightly lower when nanocrystals of EMT-type zeolite are used. As

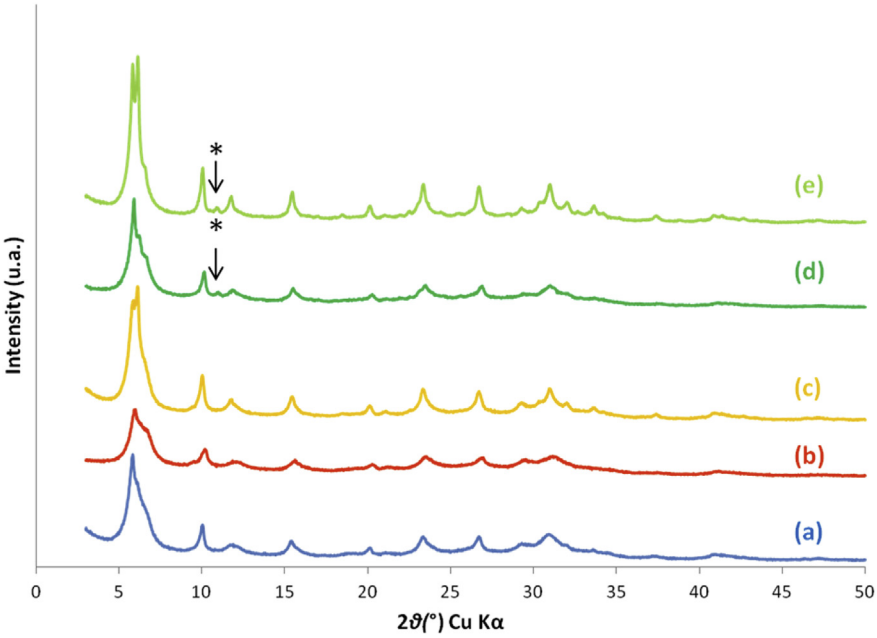

Fig. 7. XRD patterns of the zeolite samples synthesized in the presence of 5 equivalents of TEA additive and in the absence of seeds ((a), $S_{1;5;7;0}$), in the presence of 2 wt % ((b), $S_{1;5;7;2N}$) or 4 wt % ((c), $S_{1;5;7;4N}$) of EMC-2 nanocrystal seeds, and in the presence of 2 wt % ((d), $S_{1;5;7;2B}$) or 4 wt % ((e), $S_{1;5;7;4B}$) of EMC-2 conventional big crystals after 7 days of thermal treatment. *: diffraction peak that is also attributed to EMT-type zeolite ($2\theta = 10.55°$)

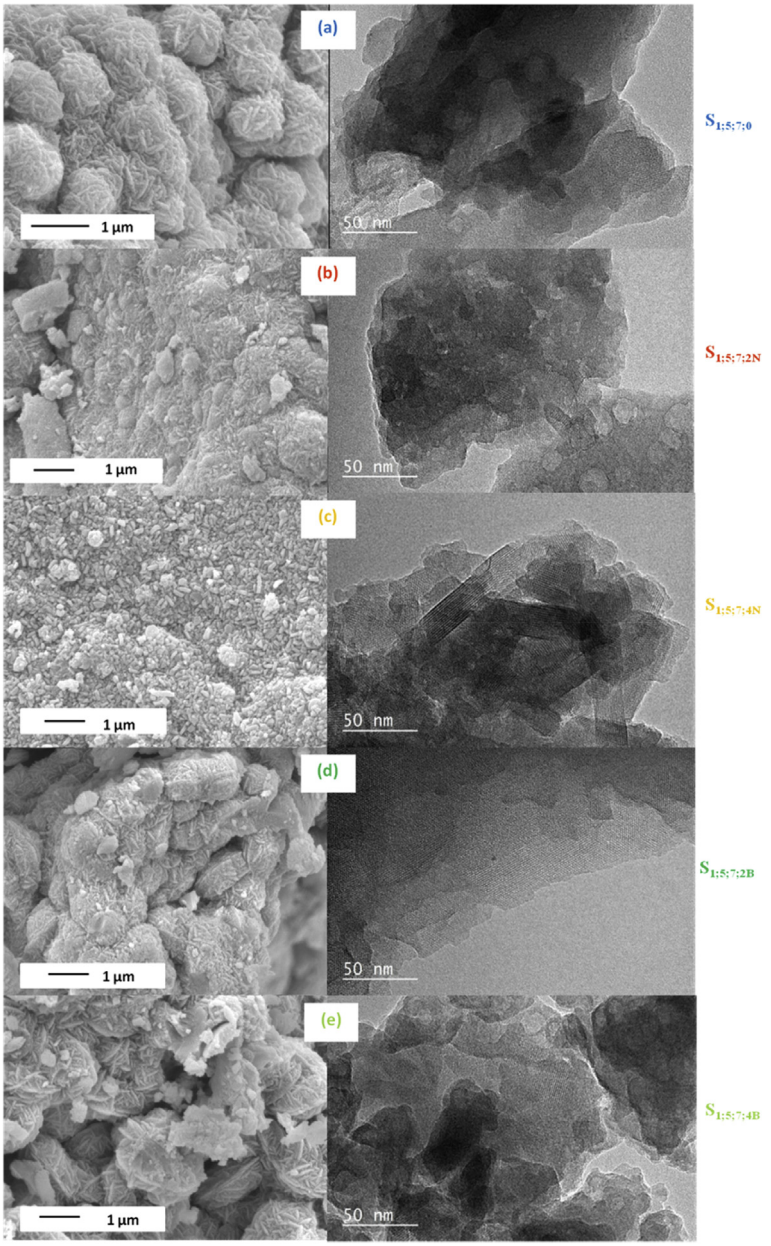

Fig. 8. SEM images (on the left) and TEM images (on the right) of the zeolite samples synthesized in the presence of 5 equivalents of TEA additive and in the absence of seeds ((a), $S_{1;5;7;0}$), in the presence of 2 wt % ((b), $S_{1;5;7;2N}$) or 4 wt % ((c), $S_{1;5;7;4N}$) of EMC-2 nanocrystal seeds, and in the presence of 2 wt % ((d), $S_{1;5;7;2B}$) or 4 wt % ((e), $S_{1;5;7;4B}$) of EMC-2 conventional big crystals after 7 days of thermal treatment.

mentioned above, this can be explained by the presence of partially non-dissolved EMT big crystals used as seeds which increases slightly the microporous volume of the final materials.

4. Conclusion

The synthesis of EMT/FAU-type nanocrystal aggregates is possible with the introduction of 5 equivalents of TEA into the synthesis media. Two ways to increase the synthesis yields were reported. Increasing the amount of sodium aluminate induces a significant increase in the synthesis yield. However, in this case, the amount of TEA is not sufficient to completely complex all aluminum atoms and enables the aggregation of crystals which permits the filtration. The amount of TEA needed to enable the aggregation of EMT/FAU nanocrystals must be five times greater than the amount of alumina. The other way to increase the yield is to increase the thermal treatment time. This is particularly a quite interesting approach because it allows a significant increase in the synthesis yield while keeping unchanged the TEA/Al_2O_3 ratio (TEA/$Al_2O_3 = 5$) required to

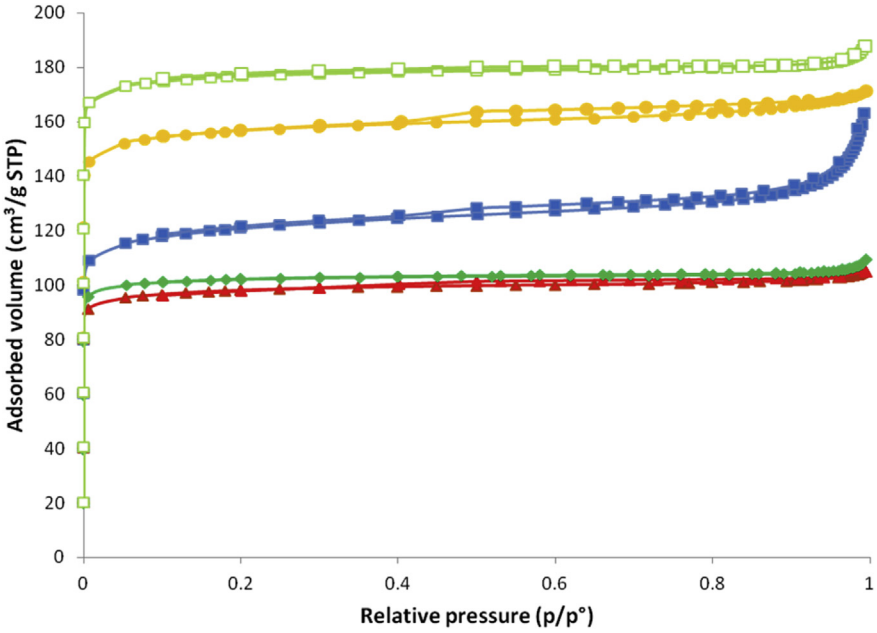

Fig. 9. Nitrogen adsorption–desorption isotherms at 77 K of the zeolite samples synthesized in the presence of 5 equivalents of TEA additive and in the absence of seeds (full square, $S_{1;5;7;0}$), in the presence of 2 wt % (full triangle, $S_{1;5;7;2N}$) or 4 wt % (full circle, $S_{1;5;7;4N}$) of EMC-2 nanocrystal seeds, and in the presence of 2 wt % (full diamond, $S_{1;5;7;2B}$) or 4 wt % (empty square, $S_{1;5;7;4B}$) of EMC-2 conventional big crystals after 7 days of thermal treatment.

allow good aggregation of EMT/FAU nanocrystals. In this case, the filtration is carried out easily.

However, the proportion of FAU-type zeolite increases with the increase of the thermal treatment time. This does not seem to be a drawback because this does not lead to a decrease of the microporous volume. In contrast, nitrogen sorption analysis shows a 50% increase of the microporous volume after a thermal treatment of 6 weeks.

Moreover, adding 4 wt % of EMT-type seeds allows an improvement of the crystalline state and an increase of the microporous volume. In that case too, compared to the non-seeded sample, a higher proportion of FAU-type zeolite is observed.

These improved simple approaches pave a new way for energy-efficient synthesis of zeolite materials for potential applications in the field of molecular decontamination and gas separation.

Acknowledgements

The authors would like to thank H. Nouali for her help in N_2 sorption analyses and L. Vidal for collecting the TEM images. A special thanks goes to the French Environment and Energy Management Agency (ADEME) and ENSCMu Foundation for their financial supports. This study is part of the Meterdiox + CORTEA funding program (Project "METERDIOX+" contract #1281C0038).

Appendix A. Supplementary data

Supplementary data related to this article can be found at http://dx.doi.org/10.1016/j.crci.2015.10.012.

References

[1] J. Caro, M. Noack, P. Kolsch, R. Schafer, Micropor. Mesopor. Mater. 38 (2000) 3.
[2] T.C. Bowen, R.D. Noble, J.L. Falconer, J. Membr. Sci. 245 (2004) 1.
[3] J. Schick, T.J. Daou, P. Caullet, J.-L. Paillaud, J. Patarin, C. Mangold-Callarec, Chem. Commun. 47 (2011) 902.
[4] P.A. Jacobs, H.K. Bayer, J. Valyon, Zeolites 1 (1981) 161.
[5] J. Dhainaut, T.J. Daou, Y. Bidal, N. Bats, B. Harbuzaru, G. Lapisardi, H. Chaumeil, A. Defoin, L. Rouleau, J. Patarin, Cryst. Eng. Comm. 15 (2013) 3009.
[6] M.E. Davis, Chem. Mater. 26 (2014) 239.
[7] M.E. Davis, M. E, Nature 417 (2002) 813.
[8] A. Corma, J. Catal. 216 (2003) 298.
[9] J.C. Jansen, J.H. Koegler, H. van Bekkum, H.P.A. Calis, C.M. van den Bleek, F. Kapteijn, J.A. Moulijn, E.R. Geus, N. van der Puil, Micropor. Mesopor. Mater. 21 (1998) 213.
[10] N. van der Puil, F.M. Dautzenberg, H. van Bekkum, J.C. Jansen, Microporous Mesoporous Mater. 27 (1999) 95.
[11] V. Sebastián, O. de la Iglesia, R. Mallada, L. Casado, G. Kolb, V. Hessel, J. Santamaría, Micropor. Mesopor. Mater. 115 (2008) 147.
[12] A.S.T. Chiang, K.J. Chao, J. Phys. Chem. Solids 62 (2001) 1899.
[13] M. Mercury, N. Zouaoui, A. Simon-Masseron, Y. Zerega, C. Reynard-Carette, R. Denoyel, M. Carette, M. Soulard, A. Janulyte, J. Patarin, Micropor. Mesopor. Mater. 177 (2013) 25.
[14] A.F. Cosseron, T.J. Daou, L. Tzanis, H. Nouali, I. Deroche, B. Coasne, V. Tchamber, Micropor. Mesopor. Mater. 173 (2013) 147.
[15] I. Kabalan, G. Rioland, H. Nouali, B. Lebeau, S. Rigolet, M.B. Fadlallah, J. Toufaily, T. Hamieh, T.J. Daou, RSC Adv. 4 (2014) 37353.
[16] N. Lauridant, T.J. Daou, G. Arnold, M. Soulard, H. Nouali, J. Patarin, D. Faye, Micropor. Mesopor. Mater. 152 (2012) 1.
[17] N. Lauridant, T.J. Daou, G. Arnold, H. Nouali, J. Patarin, D. Faye, Micropor. Mesopor. Mater. 172 (2013) 36.
[18] M. Mercury, R. Denoyel, A. Simon-Masseron, M. Carette, Y. Zerega, J. Patarin, M. Soulard, C. Reynard, A. Janulyte, Adsorption 17 (2011) 747.
[19] A. Haas, D.A. Harding, J.R.D. Nee, Micropor. Mesopor. Mater. 28 (1999) 325.
[20] T.J. Daou, N. Lauridant, G. Arnold, L. Josien, D. Faye, J. Patarin, Chem. Eng. J. 234 (2013) 66.

[21] J. Dhainaut, T.J. Daou, A. Chappaz, N. Bats, B. Harbuzaru, G. Lapisardi, H. Chaumeil, A. Defoin, L. Rouleau, J. Patarin, Micropor. Mesopor. Mater. 174 (2013) 117.
[22] E.J.P. Feijen, K. De Vadder, M. Bosschaerts, J.L. Lievens, J.A. Martens, P.J. Grobet, P.A. Jacobs, J. Am. Chem. Soc. 116 (1994) 2950.
[23] C. Baerlocher, L.B. McCusker, R. Chiappetta, Microporous Mater. 2 (1994) 269.
[24] F. Dougnier, J. Patarin, J.L. Guth, D. Anglerot, Zeolites 12 (1992) 160.
[25] F. Delprato, L. Delmotte, J.L. Guth, L. Huve, Zeolites 10 (1990) 546.
[26] M.M.J. Treacy, J.B. Higgins, Collection of Simulated XRD Powder Patterns for Zeolites, 5th revised ed., Elsevier, 2007, p. 7.
[27] E.P. Ng, D. Chateigner, T. Bein, V. Valtchev, S. Mintova, Science 335 (2012) 70.
[28] L. Bullot, B. Mulot, A. Simon-Masseron, T.J. Daou, G. Chaplais, J. Patarin, Micropor. Mesopor. Mater. 210 (2015) 194.
[29] A. Inayat, I. Knoke, E. Spiecker, W. Schwieger, Angew. Chem. Int. Ed. 51 (2012) 1962.
[30] G. Scott, A.G. Dixon Jr., A. Sacco, R.W. Thompson, Stud. Surf. Sci. Catal. 49 (1989) 363.
[31] G. Scott, R.W. Thompson, A.G. Dixon Jr., A. Sacco, Zeolites 10 (1990) 44.
[32] J.F. Charnell, J. Cryst. Growth 8 (1971) 291.
[33] C. Berger, R. Glaser, R.A. Rakoczy, J. Weitkamp, Micropor. Mesopor. Mater. 83 (2005) 333.
[34] A.A. Naiini, J. Pinkas, W. Plass, V.G. Young, J.G. Verkade, Inorg. Chem. 33 (1994) 2137.
[35] M.M.J. Treacy, J.M. Newsam, M.W. Deem, Proc. Soc. Ser. 433 (1991) 499.
[36] K. Iyoki, K. Itabashi, T. Okubo, Micropor. Mesopor. Mater. 189 (2014) 22.
[37] C.S. Cundy, P.A. Cox, Micropor. Mesopor. Mater. 82 (2005) 1.
[38] B. Zheng, Y. Wan, W. Yang, F. Ling, H. Xie, X. Fang, H. Guo, Chin. J. Catal. 35 (2014) 1800.
[39] S. Gonthier, R.W. Thompson, Stud. Surf. Sci. Catal. 85 (1994) 43.
[40] G.T. Kerr, J. Phys. Chem. 70 (1966) 1047.
[41] Y.V. Mirskii, V.V. Pirozhkov, Russ. J. Phys. Chem. 44 (1970) 1508.
[42] J. Warzywoda, R.W. Thompson, Zeolites 11 (1991) 577.